Science of the Total Environment 743 (2020) 140758

Contents lists available at ScienceDirect

Science of the Total Environment

journal homepage: www.elsevier.com/locate/scitotenv

Impact of quarantine measures on chemical compositions of $PM_{2.5}$ during the COVID-19 epidemic in Shanghai, China

Hui Chen [a,b], Juntao Huo [c], Qingyan Fu [c], Yusen Duan [c], Hang Xiao [d], Jianmin Chen [a,d,b,*]

[a] *Shanghai Key Laboratory of Atmospheric Particle Pollution and Prevention (LAP³), Department of Environmental Science & Engineering, Institute of Atmospheric Sciences, Fudan University, Shanghai 200438, China*

[b] *Institute of Eco-Chongming (IEC), 20 Cuiniao Rd., Chenjia Zhen, Chongming, Shanghai 202162, China*

[c] *Shanghai Environmental Monitor Center, Shanghai 200235, China*

[d] *Center for Excellence in Regional Atmospheric Environment, Institute of Urban Environment, Chinese Academy of Sciences, Xiamen 361021, China*

HIGHLIGHTS

- Quarantine measures led to a reduction in the concentrations of $PM_{2.5}$, SO_2, NO_x, and CO in Shanghai.
- Reduction in NO_x led to increasing O_3 and decreasing nitrate.
- Reduction in $PM_{2.5}$ is attributed to the decreasing concentrations of primary aerosols and nitrate.
- The increasing contribution of sulphate and OOA inhibited further $PM_{2.5}$ reduction.

GRAPHICAL ABSTRACT

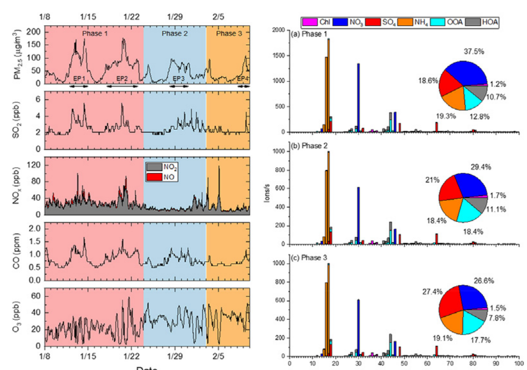

ARTICLE INFO

Article history:
Received 12 May 2020
Received in revised form 28 June 2020
Accepted 3 July 2020
Available online 6 July 2020

Keywords:
COVID-19
$PM_{2.5}$
Chemical composition
Quarantine

ABSTRACT

The COVID-19 epidemic broke out in Wuhan, Hubei in December 2019 and in January 2020 and was later transmitted to the entire country. Quarantine measures during Chinese New Year effectively alleviated the spread of the epidemic, but they simultaneously resulted in a decline in anthropogenic emissions from industry, transportation, and import and export of goods. Herein, we present the major chemical composition of non-refractory $PM_{2.5}$ (NR-$PM_{2.5}$) and the concentrations of gaseous pollutants in an urban site in Shanghai before and during the quarantine period of the COVID-19 epidemic, which was Jan. 8—23 and Jan. 24—Feb. 8, respectively. The observed results show that the reduction in $PM_{2.5}$ can be mainly attributed to decreasing concentrations of nitrate and primary aerosols. Nitrate accounted for 37% of NR-$PM_{2.5}$ before the quarantine period when there was no emission reduction. During the quarantine period, the nitrate concentration decreased by approximately 60%, which is attributed to a reduction in the NO_x concentration. Ammonium, as the main balancing cation, showed an approximately 45% simultaneous decrease in concentration. The concentrations of chloride and hydrocarbon-like organic aerosols from primary emissions also declined due to limited human activities. By contrast, sulphate and oxygenated organic aerosols showed a slight decrease in concentration, with their contributions increasing to 27% and 18%, respectively, during the quarantine period, which resulted in two pollution episodes with $PM_{2.5}$ exceeding 100 μg/m³. This study provides a better understanding of the impact of quarantine measures on variations of the $PM_{2.5}$ concentration and chemical compositions. Atmospheric oxidation capacities based on the oxidant ($O_x = O_3 + NO_2$) and oxidation ratios have been discussed for elucidating the source and

* Corresponding author at: Shanghai Key Laboratory of Atmospheric Particle Pollution and Prevention (LAP³), Department of Environmental Science & Engineering, Institute of Atmospheric Sciences, Fudan University, Shanghai 200438, China.
E-mail address: jmchen@fudan.edu.cn (J. Chen).

https://doi.org/10.1016/j.scitotenv.2020.140758

formation of haze in an environment with lower anthropogenic emissions. With increasing contribution of secondary aerosols, lower NO_x and nitrate concentrations did not completely avoid haze in Shanghai during the epidemic.

1. Introduction

In December 2019 and in January 2020, a cluster of COVID-19 cases was reported in Wuhan, Hubei, China (Li et al., 2020). COVID-19 is confirmed to transmit between humans through respiratory droplets. Liu et al. (2020) recently found that RNA of COVID-19 was detectable in aerosols in two Wuhan hospitals. To slow down the spread of COVID-19, the Chinese government issued strict quarantine measures (lockdown) in Wuhan on Jan. 23, 2020 and enacted corresponding restrictive measures in different regions according to the level of the epidemic. These measures included reducing public transportation and closing schools and business centers. These quarantine measures effectively alleviated the spread of the COVID-19 epidemic in China (Zhang et al., 2020a) but also greatly suppressed anthropogenic emissions (Wang et al., 2020a; Zhang et al., 2020b). A study in Barcelona showed that quarantine measures led to an improvement in air quality (Tobías et al., 2020). However, emission reduction did not prevent the occurrence of severe haze in China, and a plausible explanation for this is derived from a model study that showed a large emission reduction in transportation and a slight reduction in industrial production are insufficient to prevent haze in China in the winter (Wang et al., 2020a).

Air quality in Shanghai has experienced continuous, substantial improvement through the reduction of industrial emissions (Han et al., 2018). Further $PM_{2.5}$ reduction appears to be challenging, and severe haze still occasionally occurs in winter (Sun et al., 2019). Variation in the pollution levels during Chinese New Year (abbr. CNY, also known as Spring Festival) has attracted great attention because of the complex effect of anthropogenic activities on emissions. Around the CNY holiday, great amounts of migrant residents return to their hometowns to reunite with their families, which causes extremely high traffic flows. Meanwhile, anthropogenic emissions reduce to some extent because of the temporary and partial closure of factories. The concentration of pollutants usually drops during CNY and rapidly recovers during the post-CNY period (Huang et al., 2012a). Additionally, intensive fireworks activity can cause severe haze during CNY. Thus, a strict fireworks ban enacted in 2014 has helped to reduce fireworks emission during CNY (Yao et al., 2019).

Because of the joint effect of the quarantine measures and CNY holiday, emission reduction due to suppressed human activities lasted sufficiently longer in 2020, and its impact on the air quality was more distinct. In this study, we present the major chemical composition of $PM_{2.5}$ and the concentrations of gaseous pollutants in urban Shanghai from Jan. 8 to Feb. 9 in 2020. Chloride and hydrocarbon-like organic aerosols from primary emissions can be directly influenced by the suppression of human activities, while secondary aerosols including nitrate, sulphate, ammonium, and oxygenated organic aerosols are formed through gas-to-particle transformation, which is related to their corresponding precursors and the atmospheric oxidation capacity. We investigate variations in the $PM_{2.5}$ chemical composition before, during and after the CNY holiday, which can help to elucidate the impact of quarantine measures on air quality. Atmospheric oxidation capacities based on the oxidant ($O_x = O_3 + NO_2$) and oxidation ratios have been discussed for elucidating the source and formation of haze in the environment in Shanghai with lower anthropogenic emissions.

2. Methods

A Time of Flight-Aerosol Chemical Speciation Monitor (Tof-ACSM, Aerodyne Inc.) was employed to measure the concentration of non-refractory $PM_{2.5}$ (NR-$PM_{2.5}$). The Tof-ACSM was placed on a 7-story building at the Jiangwan Campus of Fudan University (31.338° N, 121.511° E). The Tof-ACSM was equipped with a $PM_{2.5}$ aerodynamic lens and a standard vaporizer heated to 600 °C (Xu et al., 2015). Since the Tof-ACSM was only able to measure NR components evaporable at 600 °C, refractory components with higher melting points ($CaSO_4$, $CaCl_2$, $MgCl_2$, NaCl, etc.) were not detectable. This might cause an underestimation of the concentration of sulphate and chloride that originated from soil dust and/or sea spay. The hourly concentrations of chloride (Chl), nitrate (NO_3), sulphate (SO_4), ammonium (NH_4), and oxygenated and hydrocarbon-like organic aerosol (OOA and HOA) were derived from the Tof-ACSM dataset (Sun et al., 2012) and used for further investigation. $PM_{2.5}$, SO_2, NO_x, CO, and O_3 were monitored in an air quality station, Xinjiangwan station, which is 500 m away from the Tof-ACSM site. The site is located north of downtown Shanghai, on the border of the Yangpu District and Baoshan District, and close to the junction of the Huangpu River and Yangtze River (Fig. S1). Nitrogen and sulphur oxidation ratios were calculated from the molar ratios of the particulate concentration and the sum of gaseous and particulate concentrations: $NOR = m(NO_3)/[m(NO_3) + m(NO_x)]$; $SOR = m(SO_4)/[m(SO_4) + m(SO_2)]$.

The study was divided into three phases (Fig. 1) according to the level of quarantine measures in Shanghai. Phase 1 (P1) is from Jan. 8 to 23 when there were no quarantine measures. The lockdown in Wuhan and in other cities of Hubei started on Jan. 23 and the CNY holiday was extended to Feb. 2 in Shanghai. Phase 2 (P2) represents this period of the extended CNY holiday with strict quarantine measures. People in Shanghai gradually returned to normal life since Feb. 3. Because of the delayed return of migrant residents, the encouragement to work from home, and other quarantine measures, Phase 3 (P3), from Feb. 3 to 9, represents the partial resumption period. There were four typical $PM_{2.5}$ pollution episodes identified during the study (Fig. 1)—EP1 and EP2 for P1, Ep3 for P2, and EP4 for P3.

3. Results and discussion

The mean concentration of $PM_{2.5}$ during P1, P2, and P3 was 60.9 ± 42.4, 41.2 ± 26.3, and 34.0 ± 23.7 μg/m^3, respectively (Fig. 3d). The $PM_{2.5}$ concentration decreased by 33% and 44% during P2 and P3, respectively. By contrast, the SO_2 and CO concentrations slightly decreased by 15% and 22%, respectively, during P3. CO is often used as a primary emission tracer because of its relatively long lifetime against oxidation by OH radicals (DeCarlo et al., 2010). Different degrees of reduction in the concentration of CO and $PM_{2.5}$ indicated that the declining pollution level cannot be solely explained by primary emissions. Secondary aerosols generated through gas-to-particle conversion are crucial to the pollution process. Sun et al. (2019) found that, in Shanghai, the chemical transformation of gaseous pollutants to secondary inorganic aerosols leads to the explosive growth of $PM_{2.5}$ in winter. The SO_2 concentration, in the range of 1.7—5.6 ppb during the study, is comparable with that in Europe (Querol et al., 2014). Strong emission reduction measures in the industrial and residential sectors have substantially lowered the ambient SO_2 concentration in China (Zhang et al., 2019). The move-out and closure of some blast furnaces of Baosteel (the largest iron and steel producer in China) in the neighboring Baoshan District has notably improved local air quality since 2010 (Han et al., 2018). Huang et al. (2012a) observed obvious ascending trends of the SO_2 and CO concentration after the CNY holiday. The quarantine measures for the COVID-19 epidemic suppressed human activities. Thus, the

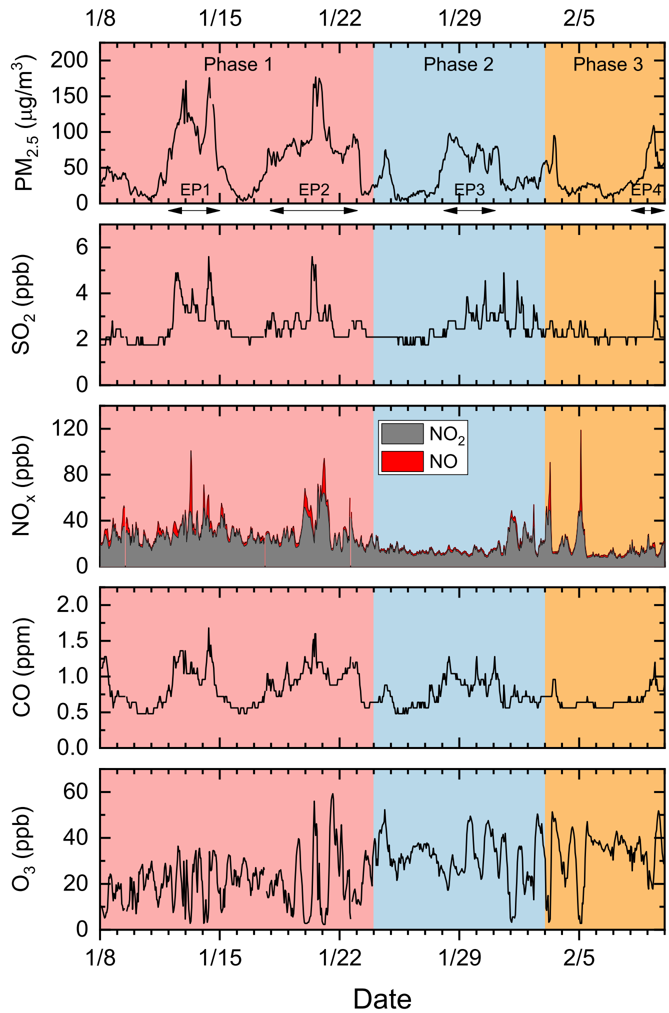

Fig. 1. Time series of $PM_{2.5}$, SO_2, NO_x (NO and NO_2), CO, and O_3 from Jan. 8 to Feb. 9 in 2020 at the Xinjiangwan air quality station in Shanghai. The three phases are presented with different background colors. Four typical $PM_{2.5}$ pollution episodes are presented with corresponding double-headed arrows.

The time series of the chemical composition of NR-$PM_{2.5}$ are presented in Fig. 2. Nitrate was the dominant contributor to NR-$PM_{2.5}$ during P1, and the nitrate concentration decreased by 55% and 60% during P2 and P3, respectively (Fig. 3e). Since NOR exhibited a slight decrease during the study (Fig. 3f), the descending NO_x concentration appeared to be the main cause for nitrate reduction during P2 and P3. Ammonium, as the main balancing cation, showed an approximately 45% simultaneous decrease in concentration during P2 and P3 in response to nitrate reduction. HOAs are mainly emitted from gasoline and diesel combustion sources (Sun et al., 2012). The HOA concentration exhibited a descending trend (Fig. 3e) because of a significant reduction in transportation during the quarantine period (Wang et al., 2020a). Biomass burning can cause pollution events during the harvest season in Yangtze River Delta (Chen et al., 2017; Du et al., 2011). Residential heating by biomass and coal is not a common activity in Shanghai in winter and primary emission from the power sector is constrained due to the implementation of “ultralow emission” standard (Zhang et al., 2019). The PMF analysis on the mass spectra does not show a significant contribution from the biomass burning and coal combustion to the $PM_{2.5}$ concentration during the campaign. Primary aerosols from fireworks used to be a dominant pollution source during CNY in Shanghai, but a strict fireworks ban enacted in 2014 has effectively reduced $PM_{2.5}$ during CNY (Yao et al., 2019). Primary aerosols from fireworks were not observed in this study.

The decreased nitrate and primary aerosols substantially reduced the $PM_{2.5}$ concentration during P2 and P3. Meanwhile, the concentrations of sulphate and OOA barely decreased, which inhibited further $PM_{2.5}$ reduction. $PM_{2.5}$ concentrations exceeding 100 μg/m^3 were observed during EP3 and EP4 (Fig. 1). EP1 and EP2 showed similar chemical proportions of NR-$PM_{2.5}$ with nitrate as the dominant contributor. During EP3 and EP4, the proportions of sulphate and OOA increased to 22.7% and 21.9%, respectively, to their maxima, while the proportion of nitrate decreased to the minimum of 28.6%. The variation of the sulphate concentration matched well with that of SOR (Fig. 3f). To further elucidate the formation mechanism of sulphate and nitrate, diurnal courses of NOR and SOR are presented in Fig. S5. NOR showed bimodal mode peaking at noon and midnight, which inferred that both photochemical and nocturnal heterogeneous reactions contributed to nitrate production. A recent study showed that photochemistry in winter can

expected increase in SO_2 and CO concentration was not observed, which was consistent with the delayed recovery of electricity demand (Fig. S4). The NO_x concentration during P1 is ~75% higher than that during P2 and P3. There were three durations with high NO_x concentration during the study. The first two durations concurred with EP1 and EP2 during P1 and the third duration occurred between P2 and P3 (Fig. 1). These NO_x peaks all arose at nights with low windspeed (Jan. 12–14, Jan. 19–21, and Jan. 31-Feb. 5 as shown in Fig. S2), which might be attributable to the local emissions from the nearby industrial parks and ports, and from the heavy duty truck transportation (Fig. S1). The third high NO_x duration, during Feb. 1 to 5, did not alter the descending trend of the NO_x concentration. A top-down study showed that NO_x emissions were significantly reduced during the CNY holiday and recovered with a slow rate afterwards (Zhang et al., 2020b). As shown in Fig. 1, NO_2 accounted for most of NO_x, which results from the fast titration of NO by O_3 and slow photodissociation of NO_2. To better elucidate the atmospheric oxidation capacity, the term oxidant ($O_x = NO_2 + O_3$) is discussed. O_x has been widely used to represent the real photochemical production of O_3 (Lu et al., 2010). The O_3 concentration showed an obvious increase with decreasing NO_x concentration during P2 and P3. In comparison, O_x concentrations showed minor differences, which indicated that the oxidation capacity during the study did not change significantly.

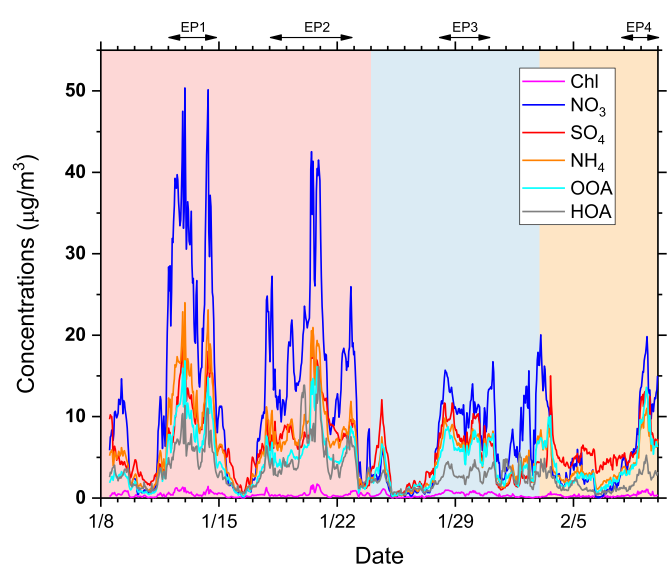

Fig. 2. Time series of the main chemical compositions of non-refractory $PM_{2.5}$. Chl, NO_3, SO_4, and NH_4 represent chloride, nitrate, sulphate, and ammonium, respectively. OOA and HOA represents oxygenated and hydrocarbon organic aerosol, which are derived from the Tof-ACSM dataset based on PMF analysis. Four typical $PM_{2.5}$ pollution episodes are presented with corresponding double-headed arrows.

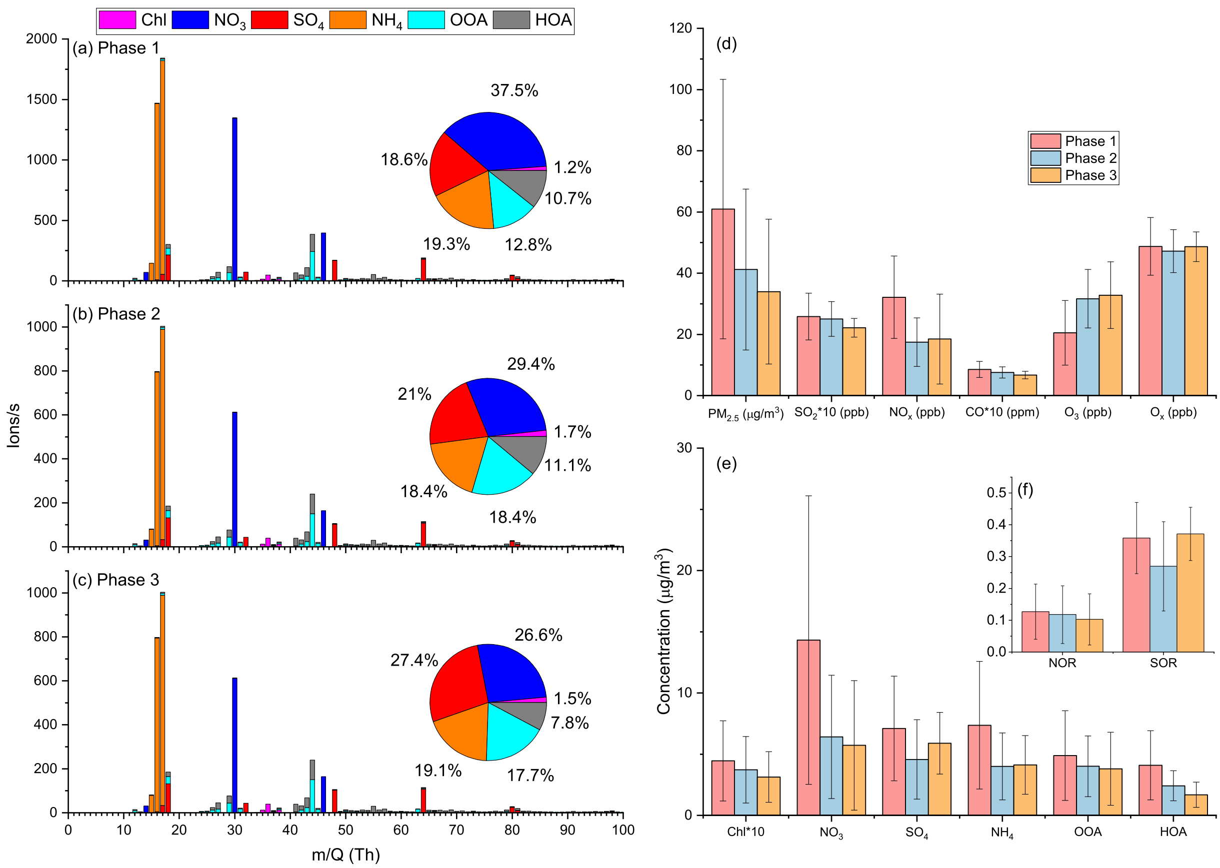

Fig. 3. Average mass spectra and corresponding chemical proportions of NR-$PM_{2.5}$ during the three phases (a–c). The mean concentration with one standard deviation of (d) $PM_{2.5}$, SO_2, NO_x, CO, O_x, (e) chloride (Chl), nitrate (NO_3), sulphate (SO_4), ammonium (NH_4), oxygenated and hydrocarbon-like organic aerosols (OOA and HOA), and (f) nitrogen and sulphur oxidation ratios (NOR and SOR) during the three phases. Note that some species are presented with different units and are multiplied by 10 for clearance, which are marked on their labels.

be as active as during the summer smog and facilitates nitrate production in China by the extremely efficient radical cycling process including volatile organic compounds (VOCs) and NO_x (Lu et al., 2019). In addition, low NO and sufficient O_3 during the night (Fig. 1) enabled nocturnal nitrate formation through the hydrolysis of N_2O_5, which has been observed in earlier study performed in Shanghai (Pathak et al., 2011). By contrast, SO_2 peaked and SOR bottomed at noon, which made it difficult to distinct the contribution of photochemical and heterogeneous reactions to sulphate production. In the photochemical reaction system, SO_2 and NO_x competes to react with OH radicals to form sulphate and nitrate, respectively. When NO_x reduced and O_x (oxidation capacity) kept constant during P2 and P3, SO_2 could participate more in photochemical reactions and form sulphate. Under low emission scenario during quarantine, the proportion of sulphate in $PM_{2.5}$ obviously increased during P2 and P3, especially when $PM_{2.5}$ concentration was low (Fig. 4). It should be noted that SOR and NOR rose simultaneously at the initial stage of EP1 and EP2, but SOR and sulphate concentration rose ahead of the occurrence of EP3 and EP4 (Fig. S5). Sulphate are hydrophilic and can promote heterogeneous reactions under humid conditions (Fu and Chen, 2017; Wang et al., 2020b). Thus, sulphate might play a more important role at the initial stage of EP3 and EP4 during quarantine period. OOA, as a surrogate of secondary organic aerosol, was correlated to nitrate and sulphate during the study (Fig. S5). The slopes between OOA and nitrate concentrations varied among different phases, and there was no clear difference in the slopes between OOA and sulphate concentrations for different phases. The formation of OOA is more complicated, but there were no collocated measurements in our study to analyze its formation mechanism. An earlier study in Shanghai with a high-resolution aerosol mass spectrometry (HR-AMS) identified semi- and low-volatility OOA (Huang et al., 2012b), which correlated with nitrate and sulphate, respectively, and the photochemical oxidation processes from HOA to SV-OOA to LV-OOA was implied as the cause of their temporal variation.

Our earlier study showed that both regional transport (windspeed >2 m/s) and stagnant weather (windspeed <2 m/s) can lead to winter haze in Shanghai (Sun et al., 2019). Descending windspeed (from 3 m/s to 0 m/s) and reducing trajectory path occurred during the pollution evolution of EP1 and EP2 (Figs. S2 & S6), which indicated regional transport initiated EP1 and EP2 and local formation maintained the pollution events until the improvement of the meteorological parameters. This is in line with a recent study indicating that surface particle pollutant can deteriorate the boundary-layer meteorological factors and lead to $PM_{2.5}$ explosive growth in Beijing (Zhong et al., 2018). As illustrated in Figs. S2 & S6, EP3 was characterized with fast windspeed and long trajectory path, and EP4 was the opposite, which indicated that EP3 and EP4 was related to regional transport and local formation, respectively.

4. Conclusion

Reduction in anthropogenic emissions during the quarantine period of the COVID-19 epidemic manifested in an obvious reduction in the concentrations of $PM_{2.5}$, SO_2, NO_x, and CO. In contrast to previous studies on the festival effect, where the pollutant concentration rapidly recovers during the post-CNY period, $PM_{2.5}$ and gaseous pollutants did not show inclining trends because of the suppression of human activities during this study. O_3 concentration did increase during the quarantine period when NO_x dropped, and the oxidant (the sum of O_3 and

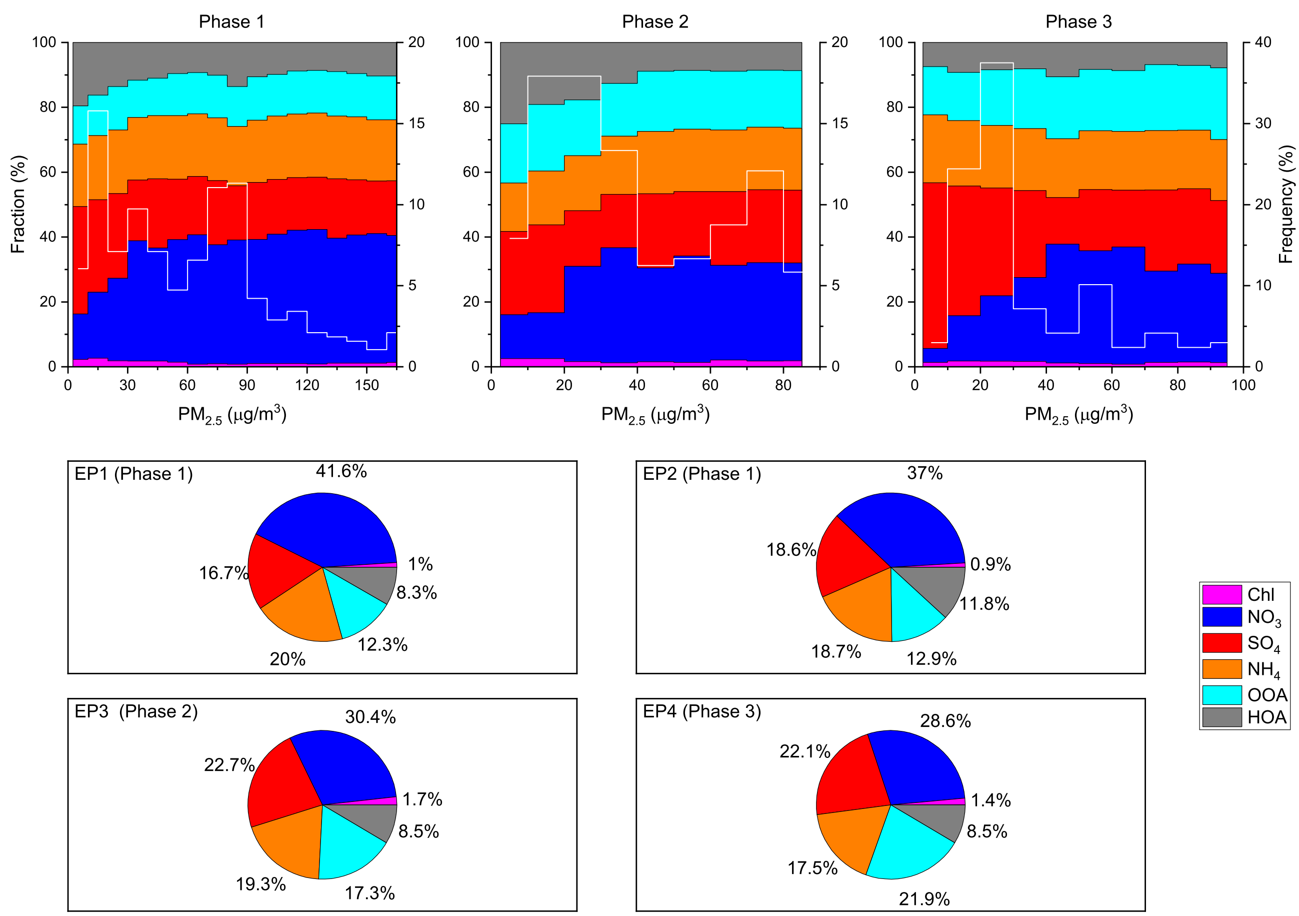

Fig. 4. Stacked fractions of the chemical compositions of non-refractory $PM_{2.5}$ (left axis) occurrence frequency (white line, right axis) under different $PM_{2.5}$ levels during the three phases. The mean proportions of the chemical compositions of non-refractory $PM_{2.5}$ during the four pollution episodes.

NO_2) did not change significantly before and during the quarantine period, which indicates a constant atmospheric oxidation capacity.

With descending SO_2 emission, nitrate displaced sulphate to be the major $PM_{2.5}$ component in Shanghai (Sun et al., 2019). Before the quarantine period, nitrate was the dominant NR-$PM_{2.5}$ component. A substantial decrease in the NO_x concentration reduced the nitrate concentration and subsequently the $PM_{2.5}$ concentration. Hence, NO_x reduction can be implemented as an effective measure for $PM_{2.5}$ control. However, a slight decrease in the concentration of sulphate and OOA inhibited further $PM_{2.5}$ reduction. Two pollution episodes with $PM_{2.5}$ concentration exceeding 100 μg/m^3 occurred during the quarantine period. Active oxidation is the hypothesized cause for fast secondary aerosol formation. Air quality has been notably improved in Shanghai by emission reduction measures (Han et al., 2018) and firework bans (Yao et al., 2019). Since the demand for economic development has increased in China, relatively high concentrations of gaseous precursors will be a huge challenge in the future. Our study shows that fast chemical transformation of gaseous pollutants to secondary aerosols could lead to air pollution even if anthropogenic activities were suppressed to a great extent. In addition to emission reduction measures, understanding the atmospheric oxidation process with respect to secondary aerosol formation should be given more attention.

CRediT authorship contribution statement

Hui Chen: Data curation, Visualization, Writing - original draft. **Juntao Huo:** Validation, Writing - review & editing. **Qingyan Fu:** Validation, Writing - review & editing. **Yusen Duan:** Validation, Writing - review & editing. **Hang Xiao:** Funding acquisition, Writing - review & editing. **Jianmin Chen:** Supervision, Writing - original draft.

Declaration of competing interest

The authors declare that they have no known competing financial interests or personal relationships that could have appeared to influence the work reported in this paper.

Acknowledgement

This work was supported by the National Natural Science Foundation of China (21806020, 91843301, 91743202, 41805091), Ministry of Science and Technology of China (2016YFC0202700), Institute of Eco-Chongming (ECNU-IEC-202001) and Marie Skłodowska-Curie Actions (690958-MARSU-RISE-2015).

Appendix A. Supplementary data

Supplementary data to this article can be found online at https://doi.org/10.1016/j.scitotenv.2020.140758.

References

Chen, J., Li, C., Ristovski, Z., Milic, A., Gu, Y., Islam, M.S., et al., 2017. A review of biomass burning: emissions and impacts on air quality, health and climate in China. Sci. Total Environ. 579, 1000–1034.

DeCarlo, P.F., Ulbrich, I.M., Crounse, J., de Foy, B., Dunlea, E.J., Aiken, A.C., et al., 2010. Investigation of the sources and processing of organic aerosol over the Central Mexican

Plateau from aircraft measurements during MILAGRO. Atmos. Chem. Phys. 10, 5257–5280.
Du, H., Kong, L., Cheng, T., Chen, J., Du, J., Li, L., et al., 2011. Insights into summertime haze pollution events over Shanghai based on online water-soluble ionic composition of aerosols. Atmos. Environ. 45, 5131–5137.
Fu, H.B., Chen, J.M., 2017. Formation, features and controlling strategies of severe haze-fog pollutions in China. Sci. Total Environ. 578, 121–138.
Han, T., Yao, L., Liu, L., Xian, A., Chen, H., Dong, W., et al., 2018. Baosteel emission control significantly benefited air quality in Shanghai. J. Environ. Sci. 71, 127–135.
Huang, K., Zhuang, G., Lin, Y., Wang, Q., Fu, J.S., Zhang, R., et al., 2012a. Impact of anthropogenic emission on air quality over a megacity - revealed from an intensive atmospheric campaign during the Chinese Spring Festival. Atmos. Chem. Phys. 12, 11631–11645.
Huang, X.F., He, L.Y., Xue, L., Sun, T.L., Zeng, L.W., Gong, Z.H., et al., 2012b. Highly time-resolved chemical characterization of atmospheric fine particles during 2010 Shanghai World Expo. Atmos. Chem. Phys. 12, 4897–4907.
Li, Q., Guan, X., Wu, P., Wang, X., Zhou, L., Tong, Y., et al., 2020. Early transmission dynamics in Wuhan, China, of novel coronavirus–infected pneumonia. N. Engl. J. Med. 382, 1199–1207.
Liu, Y., Ning, Z., Chen, Y., Guo, M., Liu, Y., Gali, N.K., et al., 2020. Aerodynamic analysis of SARS-CoV-2 in two Wuhan hospitals. Nature 582, 557–560. https://doi.org/10.1038/s41586-020-2271-3.
Lu, K., Zhang, Y., Su, H., Brauers, T., Chou, C.C., Hofzumahaus, A., et al., 2010. Oxidant (O3 + NO2) production processes and formation regimes in Beijing. J. Geophys. Res. Atmos. 115.
Lu, K., Fuchs, H., Hofzumahaus, A., Tan, Z., Wang, H., Zhang, L., et al., 2019. Fast photochemistry in wintertime haze: consequences for pollution mitigation strategies. Environ. Sci. Technol. 53, 10676–10684.
Pathak, R.K., Wang, T., Wu, W.S., 2011. Nighttime enhancement of PM2.5 nitrate in ammonia-poor atmospheric conditions in Beijing and Shanghai: plausible contributions of heterogeneous hydrolysis of N2O5 and HNO3 partitioning. Atmos. Environ. 45, 1183–1191.
Querol, X., Alastuey, A., Pandolfi, M., Reche, C., Pérez, N., Minguillón, M.C., et al., 2014. 2001–2012 trends on air quality in Spain. Sci. Total Environ. 490, 957–969.
Sun, Y., Wang, Z., Dong, H., Yang, T., Li, J., Pan, X., et al., 2012. Characterization of summer organic and inorganic aerosols in Beijing, China with an aerosol chemical speciation monitor. Atmos. Environ. 51, 250–259.
Sun, W., Wang, D., Yao, L., Fu, H., Fu, Q., Wang, H., et al., 2019. Chemistry-triggered events of PM2.5 explosive growth during late autumn and winter in Shanghai, China. Environ. Pollut. 254, 112864.
Tobías, A., Carnerero, C., Reche, C., Massagué, J., Via, M., Minguillón, M.C., et al., 2020. Changes in air quality during the lockdown in Barcelona (Spain) one month into the SARS-CoV-2 epidemic. Sci. Total Environ. 726, 138540.
Wang, P., Chen, K., Zhu, S., Wang, P., Zhang, H., 2020a. Severe air pollution events not avoided by reduced anthropogenic activities during COVID-19 outbreak. Resour. Conserv. Recycl. 158, 104814.
Wang, Y., Chen, Y., Wu, Z., Shang, D., Bian, Y., Du, Z., et al., 2020b. Mutual promotion between aerosol particle liquid water and particulate nitrate enhancement leads to severe nitrate-dominated particulate matter pollution and low visibility. Atmos. Chem. Phys. 20, 2161–2175.
Xu, L., Suresh, S., Guo, H., Weber, R.J., Ng, N.L., 2015. Aerosol characterization over the southeastern United States using high-resolution aerosol mass spectrometry: spatial and seasonal variation of aerosol composition and sources with a focus on organic nitrates. Atmos. Chem. Phys. 15, 7307–7336.
Yao, L., Wang, D.F., Fu, Q.Y., Qiao, L.P., Wang, H.L., Li, L., et al., 2019. The effects of firework regulation on air quality and public health during the Chinese Spring Festival from 2013 to 2017 in a Chinese megacity. Environ. Int. 126, 96–106.
Zhang, Q., Zheng, Y., Tong, D., Shao, M., Wang, S., Zhang, Y., et al., 2019. Drivers of improved PM2.5 air quality in China from 2013 to 2017. Proc. Natl. Acad. Sci. 116 (49), 24463–24469. https://doi.org/10.1073/pnas.1907956116.
Zhang, J., Litvinova, M., Wang, W., Wang, Y., Deng, X., Chen, X., et al., 2020a. Evolving epidemiology and transmission dynamics of coronavirus disease 2019 outside Hubei province, China: a descriptive and modelling study. Lancet Infect. Dis.
Zhang, R., Zhang, Y., Lin, H., Feng, X., Fu, T.-M., Wang, Y., 2020b. NOx emission reduction and recovery during COVID-19 in East China. Atmosphere 11, 433.
Zhong, J., Zhang, X., Dong, Y., Wang, Y., Liu, C., Wang, J., et al., 2018. Feedback effects of boundary-layer meteorological factors on cumulative explosive growth of PM2.5 during winter heavy pollution episodes in Beijing from 2013 to 2016. Atmos. Chem. Phys. 18, 247–258.